12

SELF-ASSEMBLY OF SUPRAMOLECULAR NANOSTRUCTURES: ORDERED ARRAYS OF METAL IONS AND CARBON NANOTUBES

Mario Ruben

12.1. INTRODUCTION

The use of molecular units within information processing algorithms and devices involves the controlled handling of molecules within the nanoworld. Working at the lower nanometer limit, the combination of scanning probe techniques with bottom-up self-assembly concepts has been proven to be a pivotal tool for such handling. Because such ‘‘nano-handling’’ deals with the investigation of physical phenomena close to their intrinsic correlation lengths, new ideas in terms of computing concepts may spring up from such scientific work. The perspectives emerging from nonbinaric logics by using ion dots instead of the larger quantum dots are discussed: the use of molecules within the cellular automata scheme; propositions for molecular quantum computing concepts; and the impact of surface-confined self-assembly schemes. All four concepts overlap structurally in specific 2D arrangements, called metal ion assemblies (MIAs) and networks (MINs), which represent the material platform for such alternative computation approaches. Finally, the self-assembly of carbon nanotubes (CNTs) and their use as interface between nanoscopic molecular devices and macroscopic environment will be reviewed.

Nanoscale and Bio-Inspired Computing. Edited by Mary Mehrnoosh Eshaghian-Wilner

12.1.1. Molecules: Nanoscale and Computing

Living organisms can be considered as information processing entities designed on the base of molecules (among other views). Taking a closer look at the information processing capacities of living beings, it becomes clear that their performances are (still) superior to that of silicon-based devices. This advantage is basically founded on design principles involving, in particular, massive parallelism, high integration depth, and network-like organization (e.g., brain, nerve cells, receptors, recognition schemes), all implicating molecules. However, the difficulties in mastering the built-in complexity set the main obstacle for purely molecularly and biologically based computing devices. First, rational steps moving along this tempting road map have raised a considerable interest, mainly using DNA molecules as structural and functional base (see also Chapter 13) [1]. At this point, it has to be mentioned that the herein reviewed field of molecular computing is still in its early infancy and so marked by several teething problems, e.g., the need for a complete redesign of the communication interface with the environment and the still widely unexplored integration of molecules into electrical circuits. In addition, the use of basic building blocks of living systems in technological devices raises moral and ethical questions, which have to be addressed in parallel with the progressing scientific development of the field.

The use of molecular concepts is not only restricted to biological (here meant as living) material. Beyond this scope, the introduction of simpler, organic molecules into already established information processing paradigms of silicon technology seems to be an attractive trade off. Driven by the recent emergence and massive application of new technologies working at the lower nano-regime, a length scale which matches perfectly with the intrinsic size of organic molecules is a concept that seems to be a possible shortcut for the device development of the nearer future.

Thus, throughout this chapter, the term ‘‘biologically inspired’’ will be used in the sense that it stands for the involvement of molecules in both conventional and advanced information processing schemes (e.g., storage, logic operations, bistability). The use of molecular units within information processing algorithms and devices represents herein the introduction of molecules into the nanoworld; these units can be addressed selectively by applying suitable techniques and methods exhibiting nanometer resolution (e.g., scanning probe techniques). For this to occur, several premises have to be fulfilled on the molecule side: The (i) molecular components have to possess a physical switching property (e.g., redox, magnetic, and/or spin state transitions), and (ii) their geometry should enable a smooth arrangement in two-dimensions (2D) in order to warrant (iii) precise addressing of the single molecule components. The degree of fulfilment of these premises will set the stage for the successful integration and implementation of molecular switching units into nanostructured or even nanoscaled devices. Thus, device architectures possessing addressable nanopatterned switching units promise to serve as platforms for breakthrough solutions in view of the continuously increasing demand for increased storage capacity performances [2].

The introduction of physical switching properties into molecules is a genuine task of chemical design, while the realization of molecular 2D arrangement relies on default of top-down construction principles within the lower nanometer regime and on bottom-up approaches such as supramolecular self-assembly techniques. The pivotal experiment of single molecule addressing and switching will take advantage of cutting-edge scanning probe and other techniques provided by physicists. In this way, nanoscale molecular information storage represents an archetypical example for the need of cross-border research.

Cutting edge research in the lower nanometer regime may be suspicious of scientific discoveries at the fundamental level of knowledge because the research deals with the investigation of physical phenomena close to their intrinsic correlation lengths. Within this respect, we will discuss in the following four candidates of ‘‘more-than-Moore’’ strategies, standing for technologies that exceed the conventional state-of-the-art technological scheme [3]. The following emerging perspectives are discussed: the gloaming of nonbinaric logics by using ion dots instead of the larger quantum dots [4, 5]; the use of molecules within t he cellular automata scheme [6], propositions for molecular quantum computing concepts [7]; and the impact of surface-confined self-assembly schemes. All four concepts materialize structurally in specific 2D arrangements, called metal ion assemblies (MIAs) and networks (MINs), which represent the platform for the alternative computation approaches; they will be discussed in detail. Finally, the self-assembly of carbon nanotubes (CNTs) and their use as interface between nanoscopic molecular devices and macroscopic environment will be reviewed.

12.1.2. The Ion Dot Concept

By analogy to semiconductor quantum dots [8], a metal ion coordinated by organic ligands can be considered as a natural quantum dot, i.e., the artificial atom is replaced by a real one (Fig. 12.1). Typically, the feature size of a single quantum dot is at the very lower limit, around 10 nm.However, most are much larger. So called *ion dots*, defined as single metal ion centers surrounded by their organic ligands, are at least more than one order of magnitude smaller in size [4]. Whereas the electronic level structure of a semiconductor quantum dot is merely controlled by its geometry, the electronic levels of a coordinated metal ion are tailored through the type and the geometrical arrangement of its organic ligands.

The local distribution of electron density around the respective metal ion can be used effectively as the structural and functional base for the design of nanoscaled molecular devices. Consequently, the genuine redox, electronic, or spin states of metal ions and their explicit variability (beyond the two-level scheme) will set the base for novel kinds of multistate (meaning beyond binary logics) digital information storage and processing concepts [10].

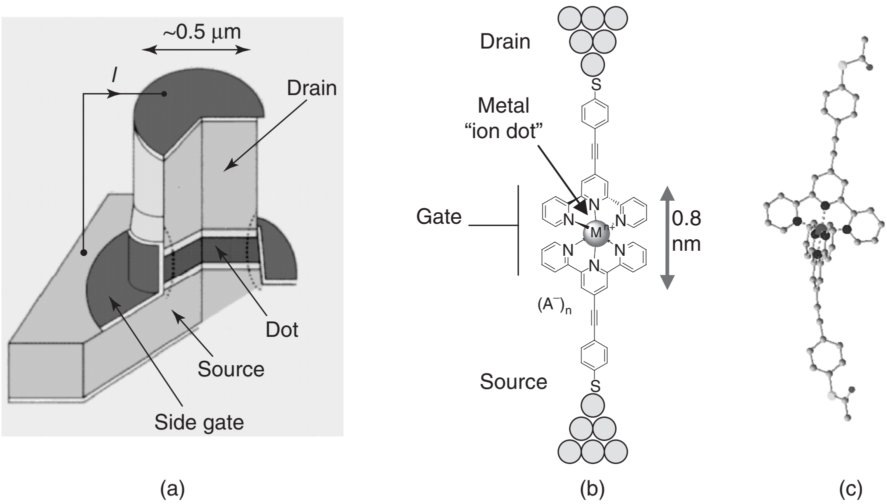

AU4 Figure 12.1. (a) Schematic representation of a typical semiconductor quantum dot showing a pillar-like structure with a typical dimension of ca. 0.5 μm [8]. (b) By analogy, the same representation exhibiting the concept of a metal ion dot. The ion dot region has an extension of ca. 0.8 nm as shown in (c) the X-ray structure of the respective Ruthenium (II) compound [9].

12.1.3. Cellular Automata Based on Molecules

Further interest in molecularly based devices has risen from an alternative encoding concept called cellular automata (see Chapter 4). Herein, molecules do not act as 0/1 switches but instead as substructured charge containers with changing local electron density distribution [10]. First envisioned for 2D assemblies of quantum dots, binary information is encoded in the internal charge distribution of appropriated dot ensembles or suited molecules. Such type of molecules should possess a small number of differently charged redox centers in a geometrically well defined intramolecular configuration. In case of half-charging, each molecule (here called "cell") exhibits degenerated ground states that can be interconverted by changing external field parameter triggers. Finally, the degeneracy of the ground states of a single cell/molecule is lifted by the electrostatic interaction with the neighbouring cells (arranged in 1D, 2D, or even 3D). The removal of the degeneracy results in "1" and "0" states, which are used for computation in the usual binary way, although the logic operation depends directly on a structural parameter, i.e., the supramolecular 2D arrangement (Fig. 12.2). The critical parameter of the encoding and AU1 processing of information here is the degree of intramolecular electronic between the redox centers within the cells: They should be able to communicate, but be neither completely delocalized nor too localized. Additionally, and perhaps an even bigger challenge is the fine tuning of the intermolecular, electrostatic Coloumb interactions between the cells/molecules. Here, surface effects involving

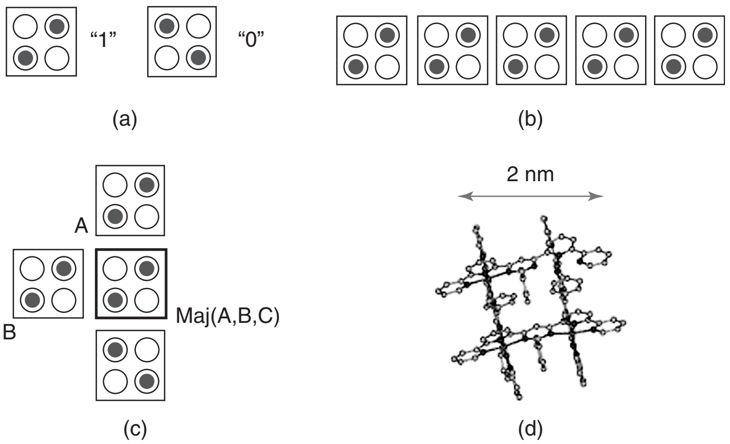

Figure 12.2. Schematic representation of the general working principle of cellular automata: (a) Coulomb repulsion keeps the electron density (dark) at antipodal sites resulting in the degenerated "1" and "0" state. (b) A wire of cellular automata can be formed by a one-dimensional arrangement of cells. The intercellular Coulomb interaction lifts the degeneracy of the 0/1 and forces all encoding units into the same state. (c) Working principle of a majority logic gate consisting of three inputs (A, B, C) which converge on an output (Maj(A;B;C;)) [6]. (d) Molecule comprised of four metal ions in a array-like configuration, which might be suited for the formation of molecule-based cellular automata by controlled formation of supramolecular 2D arrangements [10].

the underlying substrate may be very helpful to make the molecular cells communicate in the right degree. Remarkably, once the molecules are correctly charged and the intermolecular communication established, such a computing scheme does not involve any current flow.

12.1.4. Molecular Qubits

More recently, the use of molecules as quantum bits in quantum computing algorithms was proposed [7]. Quantum computers could potentially speed up certain kinds of mathematical operations by using elementary units based on quantum bits, so called qubits, instead classical binary bits. Owing to its quantum nature, a single qubit can exist in states spanning any combination of two basic wave functions $|0>$ and $|1>$. Consequently, an operation on qubit causes simultaneous operations on each of the combination's components. Thus, a single operation on a multi-qubit system can affect a huge amount of information; this is called quantum parallelism. In view of molecules, the use of either electronic states or nuclear spin states in quantum computing systems was proposed [11], whereby the primary challenge for scientists in the field lies in the maintenance of the coherence, i.e., the ability to protect the molecular system from deterioration. Among the multitude of evoked quantum computing schemes and algorithms, the implementation of Grover''s algorithm in high-spin molecules exhibiting a slow relaxation of magnetism seems to be a realistic option [12].

12.1.5. Surface-Confined Self-Assembly

There are main two ways to apply supramolecular self-assembly and self-organization techniques in order to steer of molecules on surfaces (Fig. 12.3a,b): (**a**) (i) the molecules can be pre-assembled from their components (organic compounds, metal ions, anions, etc.) under bulk conditions. (ii) Subsequently, the so formed supramolecules will be deposited on the surfaces in a second, separated step. (**b**) In a one-step-procedure, the same molecular components can be deposited altogether onto the respective surface by a surface-assisted self-assembly protocol. There, reversible, weak intermolecular forces (hydrogen bonding, metal coordination, van der Waals forces, etc.) will lead, if the molecular components are sufficiently instructed, to highly ordered surface-confined self-assembled network structures (right in Fig. 12.3). Both concepts will be discussed separately in the following two sections, whereby only highly ordered, matrix-like assemblies will be presented due to their general interests in computing concepts. It is beyond the scope of this chapter to review the more general field of surface-deposition of molecules [13]. In both approaches, straightforward scanning

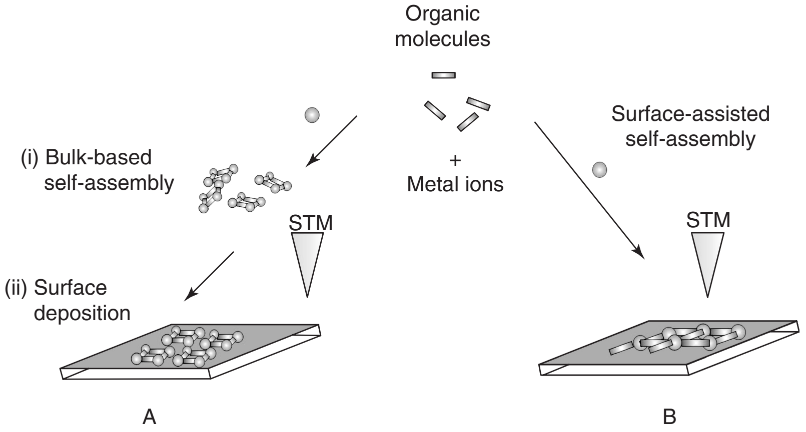

Figure 12.3. Schematic representation of the two general concepts steering the surface-confined organization of molecules and metal ions on surfaces: (A) The two-tiered approach involving (i) bulk self-assembly and (ii) surface deposition. (B) The one-step procedure of surface-assisted self-assembly by depositing organic ligands (rods) and metal ions directly on surfaces. In both approaches, scanning tunneling microscopy (STM) provides direct access to the nanodimension of the supramolecular self-organization processes.

tunneling microscopy techniques will be used to investigate the surface-confined molecular architectures. Complementary to these two concepts, some examples exhibiting the surface organization of carbon nanotubes (CNTs), which can be considered as extended 1D molecule with high aspect ratios, will be discussed.

12.2. METAL ION ARRAYS (MIAS)

12.2.1. Synthesis and Properties of Metal Ion Arrays (MIAs)

Grid-like metal ion arrays (MIAs) represent a class of coordination compounds, in which a set of metal ions is held in a matrix-like arrangement by a second set of tailor-made organic ligands. The well defined, two-dimensional (2D) arrangement of an exact number of metal ions strongly resembles the binary coded matrices and cross bar architectures used in information storage and processing technology. The metal ions at the crossing points of the finite network architecture can be supplied with well defined redox, magnetic, and spin-state transitions (all properties susceptible to use as switching parameters, either globally or locally) in a controlled manner. Furthermore, due their very distinguished rectangular geometry, such metal ion arrays might self-assemble on surfaces into extended 2D ensembles, also called ‘‘grid-of-grids’’ structures.

The design of such metal ion arrays rests on the direction of the coordination instructions, which are based on the cross-over coordination algorithms of both involved metal ions and the ligand’s coordination sites (e.g., nature, geometry, positions of the donor atoms). Therefore, the design of rectangular metal ion arrays requires perpendicular arrangements of the ligand planes at each metal center leading (depending on the topocity n and m of the ligands) to arrays structure of the $n \times m$ type (for $n = m$ to squares). According to this general procedure, metal ion arrays can be prepared in principle by careful prearrangement of the subunits using any set of metal ions and organic ligands, which opens access to a high structural and functional flexibility.

The synthesis of the metal ion arrays follows a mixed synthetic/self-assembly protocol. The organic ligands (rods in Fig. 12.3) are synthesized by conventional synthetic procedures, mainly heterocyclic chemistry. It is important that these well established techniques allow for the deliberate choice of combinations of donor atoms (e.g., N, O, P, etc.) positioned in different overall geometric environments, a necessary perquisite for the perpendicular metal ion coordination. The organic ligands are coordinated by the respective metal ions in solution-based self-assembly processes yielding the metal ion array molecules (MIAs) as bulk after removal from the solution (see step (i) in Fig. 12.3, left). Using such a general procedure, a multitude of square-like $[n \times n]$ arrays with n up to 5, but also rectangular $[n \times m]$ and more differentiated $[p \times [n \times m]]$ metal ion architectures are currently accessible (Fig. 12.4).

Aside from their synthetic accessibility and broad variability, metal ion arrays (MIAs) show very interesting physical properties in light of their potential to

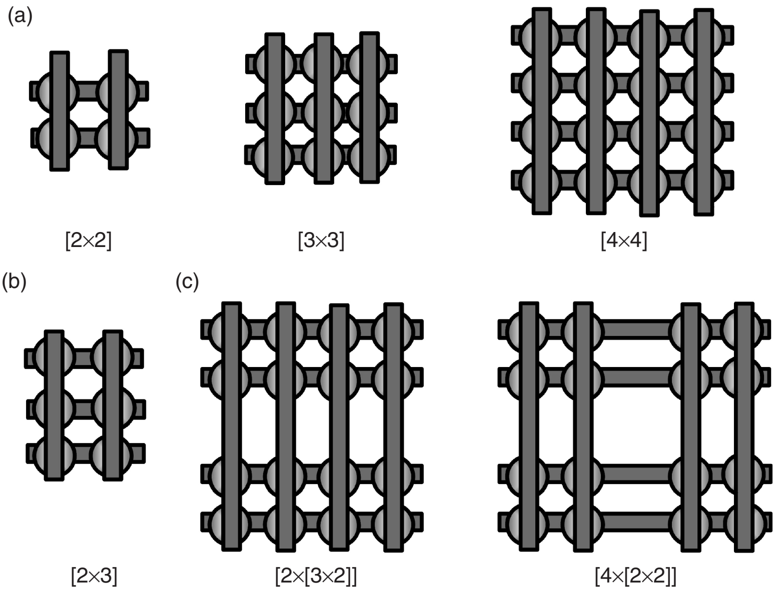

Figure 12.4. The different types of metal ion arrays (MIAs): (a) [2 × 2], [3 × 3], and [4 × 4] squares, (b) [2 × 3] rectangles and (c) some examples of more complex architectures of the [2 x [4 × 2]] and [4 x [2 × 2]] type (reprinted from [10]).

enable bi- or even multistability at the nanometer scale. Among the promising molecular parameters, the redox and the magnetic behavior of some [2 × 2] and [3 × 3] metal ion arrays have been studied in detail.

In their bulk, some [2 × 2] Co_4^{II} and [3 × 3] Mn_9^{II} arrays have been proven to be very efficient electron reservoirs exhibiting multiple, partially one-electron, reduction, and oxidation steps in diluted solutions [14]. The [2 × 2] Co_4^{II} metal ion array exhibit very extraordinary reduction behavior in multiple (up to twelve), well resolved single electron steps with wave separations between 20 to 40 mV (Fig. 12.5a). Rather low redox potentials (under 3 V) guarantee robust cycling for some Co_4^{II} compounds; this is a necessary prerequisite for low fatigue rates in future device stability. Note the stability of the recuced species can be directly AU2 correlated to the nature of the organic ligands and the metal ions, since replacing the Co^{2+} ions by Fe^{2+}, Zn^{2+}, Mn^{2+} reduces the cyclability considerably [15]. In view of the realization of molecular cellular automata (see Chapter 4), two basic results dealing with metal ion arrays of the [2 × 2]Co family might be of interest: (i) The metal ion arrays can be ordered along step edges of graphite into 1D infinite chains (Fig. 12.5b) [16]. (ii) The step-wise synthesis of a [2 × 2]$Co_2^{II}Co_2^{III}$ metal ion array yields molecular species, which show exactly the diagonally localized electron density distribution required for the internal cell structure of such automata devices (Fig. 12.5c) [17]. However, questions concerning the degree of

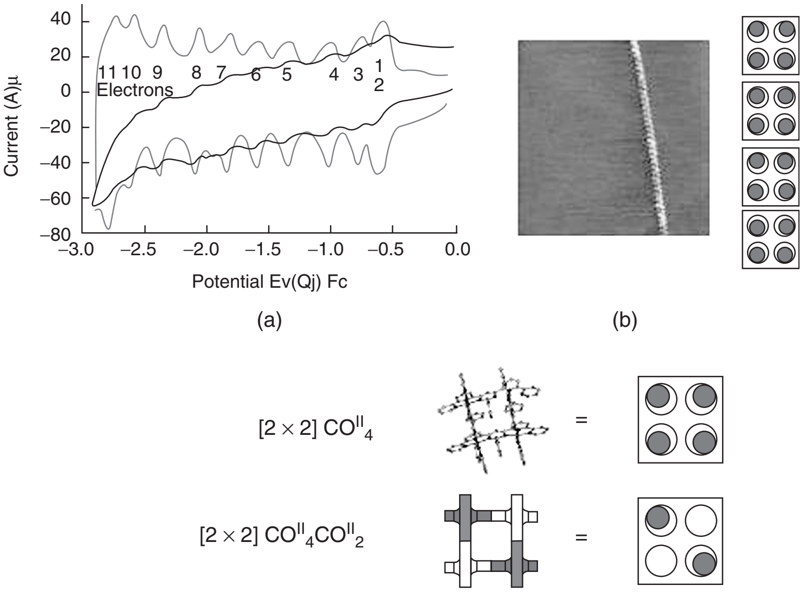

Figure 12.5. (a) Solution cyclovoltammogramm showing the well-resolved single electron reductions of a [2 × 2] Co_4^{II} metal ion array in potential window between 0 and 3 V. Below, the X-ray structure and its translation into the cellular automata symbol are shown [15a]. (b) STM image showing the aligning of the [2 × 2] Co_4^{II} metal ion arrays along the step edges of a graphite substrate after drop casting [16]. (c) Constitution and symbol of the mixed valence [2 × 2] $Co_2^{II}Co_2^{III}$ metal ion array [17].

intramolecular delocalization and the strength of the intermolecular Coloumb interaction remain to be solved before the utility of the metal ion arrays within the frame of the cellular automata concept can be proven. In addition, on the apparatus' side, single molecule techniques discriminating between the two charge states of a cell remain to be developed as feasible read-out tools.

Among the physical molecule properties that may be considered for magnetic, molecular data storage systems, the spin transition (ST) phenomenon featuring the transition between the low spin (LS) and the high spin (HS) states of Fe^{II} ions is an attractive process worth considering as the base of molecular memory effects [18]. Molecular ST systems possess a unique concomitance of possible "write" (temperature, pressure, light) and "read" (magnetic, optical) parameters [19]. Investigations along these lines revealed spin transition behavior in several [2 × 2] Fe_4^{II} metal ion arrays. The internal spin states of the incorporated Fe^{II} ions could be switched successively between their diamagnetic Fe^{II}(LS) and the paramagnetic Fe^{II}(HS) spin states by applying external field triggers (temperature, pressure, light) on macroscopic samples (Fig. 12.6) [10, 20].

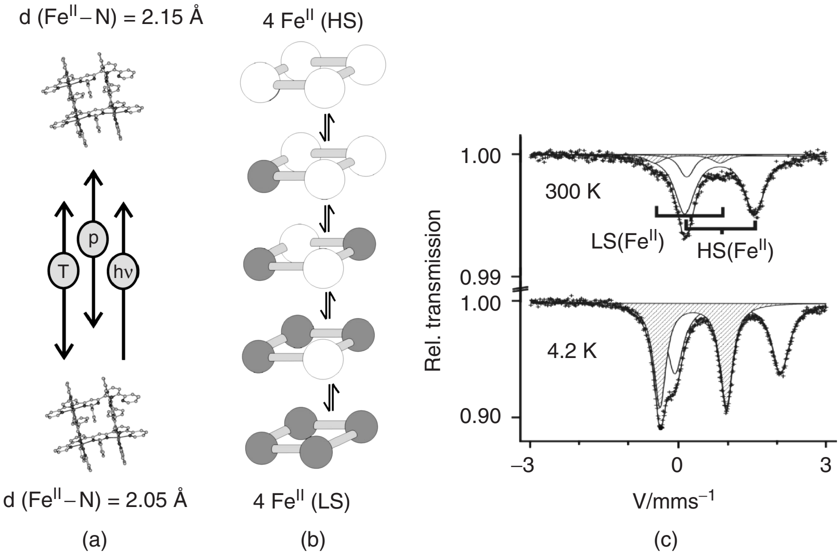

Figure 12.6. Spin transition scheme of the [2 × 2] Fe_4^{II} metal ion arrays exhibiting switching between the diamagnetic low spin (LS) and the paramagnetic high spin state. (a) and (b) The spin state change can be triggered by temperature, pressure and light; the averaged Fe-N bond lengths in the 3 HS/1 LS and in the 1 HS/3 LS states are given. (c) The Moessbauer spectra at two different temperatures showing the spin transition between the two Fe(II) species [20].

In addition, the magnetic anisotropy in a series of [2 × 2] Co_4^{II} metal ion arrays was investigated by single-crystal magnetization measurements at low temperatures. The magnetization data exhibit metamagnetic-like behavior and are explained by the weak-exchange limit of a minimal-spin Hamiltonian including Heisenberg exchange, easy-axis ligand fields, and the Zeeman term [21].

12.2.2. Surface Organization of Metal Ion Arrays (MIAs)

Supramolecular chemistry, with its characteristic control of the self-assembly process and its intrinsic defect tolerance, can be a very efficient synthetic tool to achieve ordered arrangements of metal ions with subnanometer precision [22]. In order to study supramolecular entities under restricted spatial dimensions, in particular on flat surfaces, scanning tunneling microscopy (STM) is the investigation method of choice due to its excellent real-space imaging and manipulation capabilities. Recent advances in scanning probe techniques of molecules have enabled imaging and also manipulation with partially sub-molecular resolution [13c]. Thus, after bulk self-assembly synthesis, monolayers of [2 × 2] Co_4^{II} metal ion arrays could be generated simply by drop casting the molecules on an atomically flat graphite surface (HOPG) (following way **A** in Fig. 12.3). The highly ordered supramolecular surface structures consisting of densely packed flat-lying [2 × 2] Co$_4^{II}$ metal ion arrays (MIAs) of rectangular shape are formed spontaneously from dilute acetone solution as almost defect-free domains of up to 0.5 µm^2 (Fig. 12.7). The domain growth proceeds outwards from single nucleation points, a process which might be considered as two-dimensional crystallization.

Certain substitution patterns at the organic ligands provoke on-the-edge orientation of the metal ion arrays with respect to the surface. But, most of the observed metal ion [2 × 2] arrays result in flat tiles forming a "grid-of-grids" superarray, in which the presence of the [2 × 2] metal ion grids is reflected by the 2.5 × 2.4 nm periodicity in agreement with the molecule sizes determined by X-ray crystallography [23].

It was shown that films of the pure [2 × 2] Co$_4^{II}$ metal ion arrays are poorly conductive, but doping them with an excess of cadmium (II) ions could increase the conductivity up to $10^{-2}\,\mathrm{S\,cm^{-1}}$ [24]. In similar ways, [3 × 3] Mn$_9^{II}$ metal ion arrays were deposited on both HPOG and Au(1 1 1) surfaces [25]. By application of a voltage pulse through the STM-tip on the monolayer of metal ion arrays, a single [2 × 2] Co$_4^{II}$ metal ion array could be lifted, leaving a square-like hole of the dimension of the molecule (see Fig. 12.7b). The migration rate of the hole was measured to be 200 times slower than in a monolayer of cycloalkanes, reflecting the degree of adsorption of the molecules to the graphite surface [23].

Further insight into the intramolecular electronic situation of isolated single [2 × 2] Co$_4^{II}$ metal ion arrays at room temperature and ambient conditions could

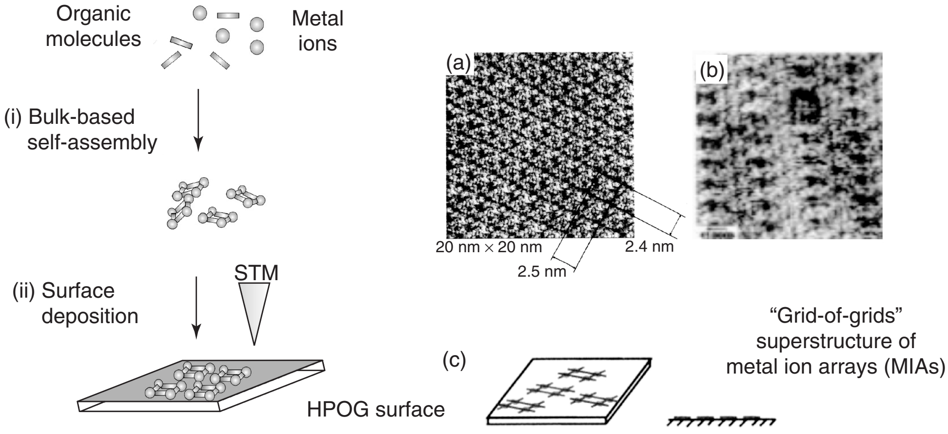

Figure 12.7. Schematic representation of the deposition of metal ion arrays (MIAs) on surfaces: (a) STM image of the monolayer of [2 × 2] Co$_4^{II}$ metal ion arrays on graphite. The periodicity of the grid-of-grids network is shown with 2.5 × 2.4 nm. (b) A hole in the supramolecular monolayer is produced by potential induced lifting of a single [2 × 2] Co$_4^{II}$ molecule with the STM tip. (c) Schematic representation of the disposition of the MIAs at the surface (top and side view) [23].

be gained by a scanning tunneling spectroscopy technique called current induced tunneling spectroscopy (CITS) [26]. The experiments allowed the localization of the positions of the incorporated $\mathrm{Co^{II}}$ ions by a selective mapping of the highest occupied molecular orbitals (HOMOs). Principle density functional theory calculations confirmed that in this type of molecules the HOMOs possess a large d-character, such that they are strongly localized around the positions of the metal ions. Consequently, the projection (of the CITS maps at certain negative tunneling biases) indicates electronically the cornerstone positions of the four $\mathrm{Co^{II}}$ metal ions (Fig. 12.8) [10]. The same technique was successfully applied to the higher homologous $[3 \times 3]$ $\mathrm{Mn_9}^{\mathrm{II}}$ and $[4 \times 4]$ $\mathrm{Mn_{16}}^{\mathrm{II}}$ MIAs aligning respectively 9 and 16 manganese metal ions. The obtained CITS maps mirror the structural situation within the metal ion arrays; although very regularly arranged, the metal ions display in these higher homologues a more lozenge-like structure (Fig. 12.8). This structural deviation from the optimal square-like arrangement can be attributed to the ‘‘pinching-in’’ of the organic ligands during metal ion coordination, reflecting the importance and the consequences of sufficiently instructed metal–ligand interactions for the outcome the self-assembly processes [25].

In conclusion, the formation of highly ordered 2D monolayers of metal ion arrays on surfaces represents a two-tiered self-assembly process: (i) The $[n \times n]$ metal ion arrays are formed in a bulk self-assembly step in solution from their molecular components (organic ligands and metal ions). Subsequently, (ii) the $[n \times n]$ metal ion arrays are self-assembled themselves into densely packed domains of monolayers on the graphite surface. The first self-assembly process relies on the read-out of the coordination instructions stored in the ligands and the metal ions, while the second is steered by van der Waals forces between the metal ion arrays on one side and between arrays and graphite surface on the other side. Due to the flat, square-like geometry of the metal ion arrays, this second

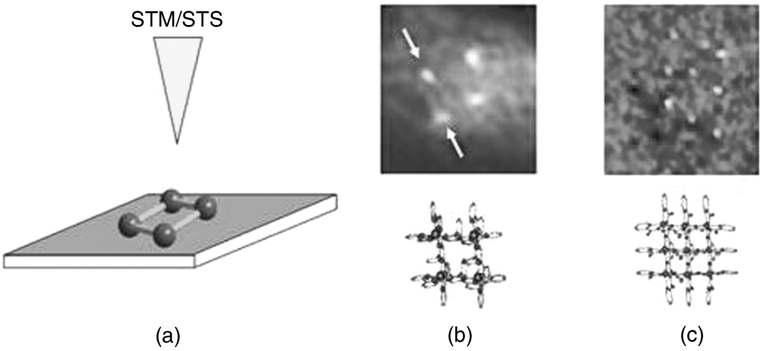

Figure 12.8. (a) Schematic principle showing the metal ion array on a graphite surface (b) and (c) the results of the locally resolved current-induced tunneling spectroscopy (CITS) measurements of a $[2 \times 2]$ $\mathrm{Co_4}^{\mathrm{II}}$ and $[3 \times 3]$ $\mathrm{Mn_9}^{\mathrm{II}}$ indicating the position and arrangement of the respective metal ions [26].

self-assembly process under 2D confinement automatically results in a highly ordered "grid-of-grids" superstructure. Consequently, monolayers of $[n \times n]$ MIAs exhibit a two-fold supramolecular matrix structure, (i) internally by the ligand-directed coordinative positioning of the metal ions and (ii) externally by the van der Waals directed formation of the "grid-of-grids" superstructure. The addressing of the single metal ion array at the single array level was achieved by removing one molecule from the monolayer with help of the scanning tunneling microscopy (STM) tip. Single metal ion addressing inside of isolated metal ion arrays could be achieved electronically through the use of scanning tunneling spectroscopy technique (CITS) [26].

12.3. METAL ION NETWORKS (MINs)

12.3.1. Surface-Confined Assembly of Metal Ion Networks (MINs)

The method **B** in Fig. 12.3 introduces a shortened conceptual alternative to the above described multistep approach in achieving extended highly ordered MIAs on surfaces. Instead to the three-tiered self-assembly approach of method **A**, metal ions and organic ligands are now self-assembled in only one self-assembly step under immediate 2D confinement of the surfaces [22]. Experimentally, the organic ligand molecules are deposited by organic molecular beam epitaxy on a metallic surface under ultra high vacuum conditions. A more or less complete organic monolayer is formed, on which the respective metal ions are subsequently co-deposited by electron beam evaporation. A short annealing period (typically several minutes) supplies the necessary mobility of the molecular components, guaranteeing the required kinetics for accomplishing the surface-assisted self-assembly process [23]. Depending on the applied molecular ligand/metal couples, regular network structures of different geometries, with domain sizes up to several hundred nanometers, are formed. Within these extended, polymeric 2D network structures, the metal ions are positioned at the crossing points in very regular distances of a few nanometers. Scanning tunneling microscopy (STM) has been proven to be the ideal tool to obtain structural information of the formed metal ion networks (MINs) structures in a straightforward way (Fig. 12.9).

One example of such a metal ion network is the self-assembly of linear dicarboxylic acid ligands with Fe(0) metal ions on a Cu(1 0 0) surface [28]. At a Fe/ligand ratio of 0.5/1, rectangular molecular assemblies could be obtained consisting of dimeric iron nods that are interconnected by an organic backbone of orthogonally arranged ligand linkers (Fig. 12.10). Within the resolution limit of the STM, the length of the Fe–O bond of the metal ion to the coordinating carboxylates was determined with d(Fe–O) = 1.9–2.3 A (an expected range for a Fe(II) species). The Fe–Fe distance within the dimeric nods was shown to be between 4.5 and 5.0 A, a value that is considerably larger than in comparable bulk structures exhibiting metal-metal bonds [28]. The coordination geometry around each iron ion can be interpreted as square-planar, which is quite unusual for

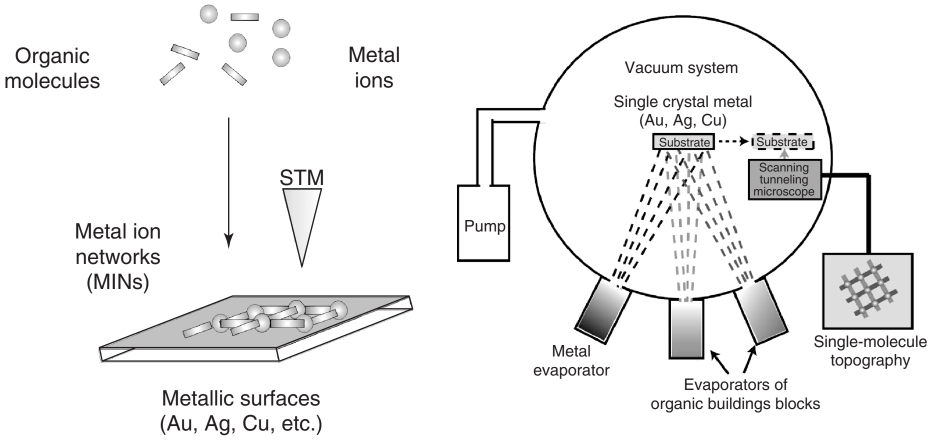

(a) (b)

Figure 12.9. (a) The scheme represents the experimental setup of the UHV-based codeposition of the molecular components (metal atoms and organic ligands) on metallic substrates. (b) The components self-assemble on metallic surfaces under UHV 2D confinement to extended metal ion networks (MINs), which can be investigated *in situ* by scanning probe techniques [27].

Iron(II) ions. However, the electronic coupling of the coordinated metal centers to the metallic substrate or possible counterbalancing of the charges of the assembled molecular structures by mirror charges within the upper layers of the metallic substrate have to be taken into consideration to explain the electronic properties of such surface-deposited metal atoms or ions [29]. Looking at the distinct metal/ ligand 2/4/2-stoicheometry around the dimeric Fe_2-nodes, it seems reasonable to believe that the principle of electro-neutrality persists under near-surface

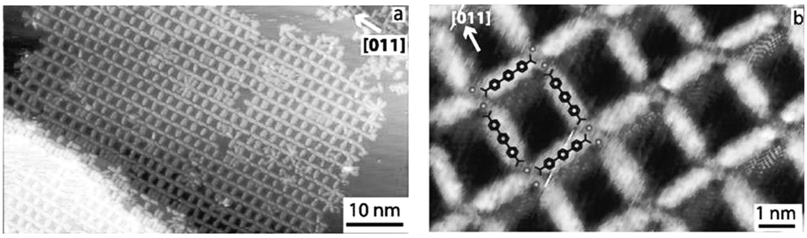

Figure 12.10. (a) STM image showing the 2D topography of the extended Fe-metal ion dicarboxylic acid network on a Cu(1 0 0) surface; (b) high resolution image of the same network indicating the positions of the organic ligand dicarboxylic acid backbone and the interconnecting dimeric Fe-nod structures [28].

conditions. Such view would lead to the definition of two Iron (II) metal ions surrounded by four deprotonated, negatively charged carboxylic groups of the interconnecting ligands. The formation of electro-neutral 4+/4-units will depend critically on the smoothness of the deprotonation reaction of the carboxylic acid groups. Alternative to the spontaneous deprotonation of carboxylic acid groups on copper surfaces, a redox reaction involving the reduction of four carboxylic protons under simultaneous oxidation of the two Iron(0) centers might be considered. The formed gaseous hydrogen could easily migrate into the UHV environment so favoring the accomplishment of the redox reaction. Furthermore, it has been mentioned that the principle of maximal occupancy of the coordination sites might not be strictly valid under 2D-UHV confinement, since the ligands tend to layer down onto the surface and additional solvent molecules, present in conventional reaction conditions, are not present to fill open coordination sites at the metal ion.

On the ligand side, it was shown that the lengths of linear rod-like ligands can be two, three, or four phenyl units without losing the self-assembly ability. Thus, the distance between the positions of two Fe-dimers within the metal ion network can be deliberately chosen between 1.2 and 2.0 nm. Near-edge, X-ray adsorption fine structure studies have shown that the aromatic backbones of the ligands are adsorbed with their phenyl rings almost parallel to the Cu(1 0 0) surface plane [28]. Besides changing the lengths, the introduction of photoactive double bond structures into the ligand backbone is possible. Interestingly, the introduction 2D prochirality on the ligand side leads to less-ordered metal ion network structures,

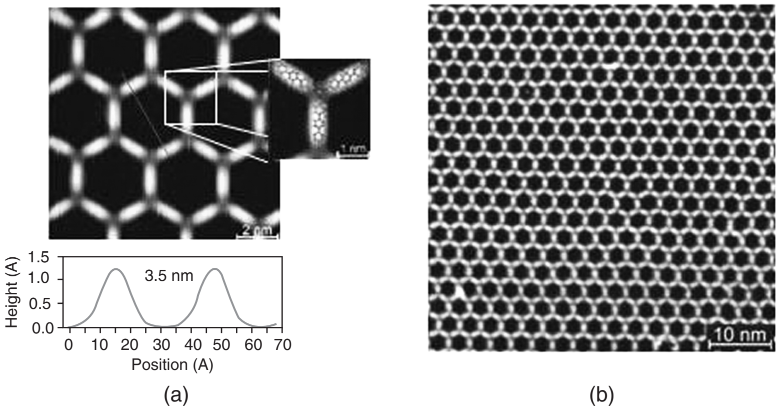

(a) (b)

Figure 12.11. (a) The high resolution STM image represents the 2D topography and the internal structure of the extended hexagonal Co-metal ion dicarbonitrile terphenyl network indicating three-fold carbonitrile coordination around monomeric Co-centers at the crossing points. Internal cavities of 3.5 A diameter are generated on the Ag(1 1 1) surface. (b) STM image showing extended regular metal ion network topology [31].

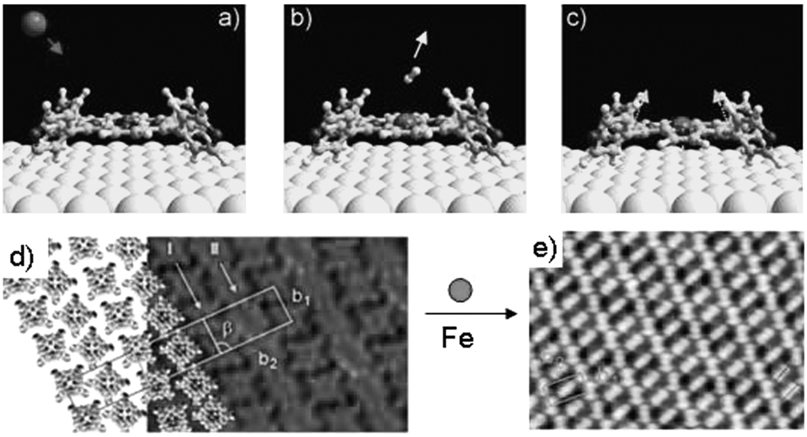

Figure 12.12. (a–c) The three main processes during the metallation of surface-deposited porphyrins on a Ag(1 1 1) surface are schematically illustrated: (a) A pure protonated porphyrin layer is exposed to an iron monomer from an atomic beam. (b) The pyrrolic protons are reduced to molecular hydrogen which desorbs while the codeposited Fe(0) is oxidized and incorporated into the dianionic porphyrinato core. (c) This process is associated with a nonplanar deformation of the porphyrin macrocycle. (e) STM image and model of the densely packed monolayer of *meso*-porphyrins on Ag(1 1 1) exhibiting the two different orientations. The models including the unit cell ($b_1 = 13.9$ Å, $b_2 = 27.4$ Å) highlight the structure and facilitate the identification of the molecular moieties. (e) STM image of the metalated monolayer showing the unaffected unit cell [32].

where the energy gain during the metal ion coordination directed self-assembly is reduced; this leads to considerably smaller domain sizes on comparable substrates [27]. Moreover, it was shown that heteroleptic metal ion networks are also accessible by replacing two dicarboxylic acid ligands with two linear pyridines [30].

The same surface-assisted self-assembly strategy can be applied to different metal ion–ligand couples. Replacing the dicarboxylic acids with linear biphenols leads to hexagonal metal ion networks now exhibiting single ion arrangement at the crossing points. By the same token, the combination of Cobalt ions with linear bis-dicarbonitrile ligands generates hexagonal networks with domains up to several nanometer domain sizes (Fig. 12.11) [31]. The symmetry of the evolving metal ion networks (MINs) has been proven to be independent from the symmetry of the substrate, so excluding mere templating effects. It was shown that intrinsic metal ion network symmetry is predominant with respect to the substrate symmetry. The match or mismatch between substrate and metal ion network symmetry is expressed by the evolving domain size and defect probability [31].

12.3.2. Filling Macrocycle Arrays

Not only linear ligands but also macrocylic ligands as porphyrines and phthalocyanines can be used in the surface-assisted self-assembly approach. Thus, *meso*-tetrapyridyl porphyrines form on Ag(1 1 1) surfaces' densely packed monolayers containing two orientations of the macrocycles (due to packing effects). Co-depositing of iron atoms onto this monolayer leads to selective incorporation of the metal atoms into the porphyrin macrocycles whereby the template structure is strictly preserved (Fig. 12.12) [32]. The immobilization of the molecular reactants allows the identification of single metalation events in a novel reaction scheme.

This ‘‘filling'' approach opens up appealing opportunities, especially because it seems to be easily applied to a large variety of porphyrin or related macrocycle species organized on surfaces (which can be metalated by iron and other metal centers). Specifically, the ‘‘filling approach'' allows the formation of low-dimensional metallo-porphyrin architectures by using preorganized immobilized macrocycle template arrangements that are subsequently functionalized by metallation. Moreover, novel porphyrin compounds can be created because procedures can be conceived where the addition of a metal center enters as a final step. Current work addresses the elucidation of the coordination characteristics of the involved metal centers, which will also set the base for the investigation of the physical properties (e.g., the magnetism) of single metal centers in the formed extended metal ion networks.

12.4. SELF-ASSEMBLY OF CARBON NANOTUBES (CNTs)

Remarkable electronic properties make carbon nanotubes (CNTs) promising building blocks for molecular or nanoscale devices. In comparison with molecules, CNTs represent an ideal link between the nanoscopic molecular world and the macroscopic implementation of possible devices involving molecules. CNTs can fulfill this role because of their typical dimensions involving both nanometer diameter and micrometer lengths. To use them in this interlinking role, CNTs need to be assembled with nanometer precision into hierarchical arrays over large scales of areas; at the same time, they to be connected to partially macroscopic device components (e.g., electrodes) [33]. At the nanoscale, different techniques are pursued to achieve highly ordered structures. Thus, most of the available methods rely on fabrication of CNTs on prepatterned substrates or catalysts [34]. In a different approach, self-assembly techniques take use of the capillary forces leading to three-dimensional micro-patterns of aligned CNT films [35]. Thereby, a water-spreading method on prepatterned substrates is used to direct the growth of highly ordered CNT films. Although this process is still restricted to the micrometer length scale, improvement of the feature resolutions seems possible (Fig. 12.13).

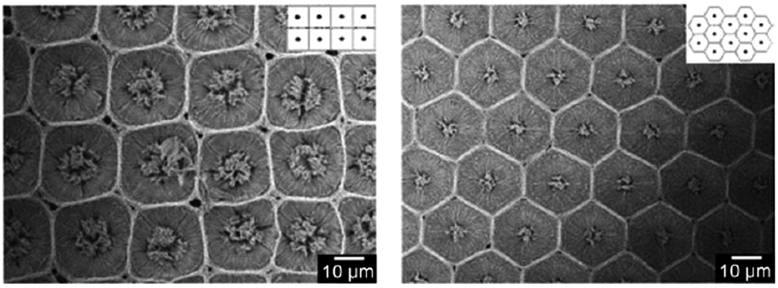

(a) (b)

Figure 12.13. Highly ordered carbon nanotube film patterns—(a) cubic and (b) hexagonal—are prepared by applying capillary forces on growing carbon nanotubes on prepatterned surfaces [35].

Within the nanometer regime, different arrangements of carbon nanotubes have achieved nanometer-scale electrodes of metals. Such controlled arrangement foreshadows the implementation of nanotubes into device architectures that interface the nano world with the macrosopic world. Some early examples make use of individual carbon nanotubes as simple quantum wires by interconnecting a pair of electrodes as depicted in Figure 12.14a [36, 37]. Based on this motif, more elaborate device structures like transistors or SQUID loops were reported (Fig. 12.14b,c) [38, 39]. The different kinds of CNT-based devices recently produced represent a tool kit to interface functional molecules directly within devices, enabling the exploitation of functionalities of molecules within the

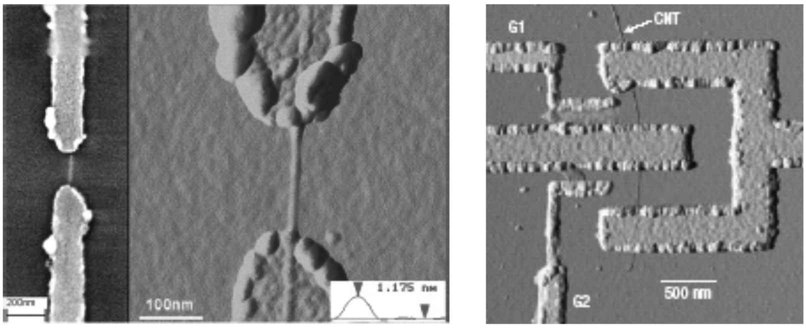

(a) (b)

Figure 12.14. (a) Scanning electron microscope (SEM) (left) and STM images (right) of an individual single wall carbon nanotube deposited onto a pair of electrodes. Inset: an AFM profile across a carbon naotube showing its thickness of 1.2 nm [37] (b) AFM image of a typical device geometry of the carbon nanotube CNT-SQUID [39].

nanoregime. To move towards this goal, it will be necessary to control the binding interaction of the respective molecules with the carbon nanotube surface selectively via suited linkers (e.g., pyrene groups).

12.5. CONCLUSION

Highly ordered supramolecular metal ion arrays (MIAs) and metal ion networks (MINs) can be constructed on surfaces by using two different general approaches: (A) a three-tiered hierarchical synthesis/self-assembly/self-assembly protocol or (B) by one-step 2D confined coordination of the metal ions/atoms through organic ligands directly under assistance of the surface. Both strategies lead to nanometer sized, highly symmetric regular arrangements of metal ions on surfaces, whereby the components (organic ligands and metal ions) can be changed in their size, identity, and electronic properties. This modular approach enables a deliberate choice of the nature as well as the relative positioning of the metal ions, in addition to the fine-tuning of their electronic environment. Remarkably, individual metal ions can be effectively imaged and addressed by scanning tunneling microscopy (STM) and spectroscopy (STS) techniques. In the future, direct addressing of electronic properties of the metal ion states (redox, spin states, magnetic anisotropy) might lead to the exploitation of bi- or even multistability at the single ion level, e.g., within the 1 nm regime. Such possibilities posit the ion dot concept in analogy to the well established quantum dot approach. In addition to the possibility of controlled nanopatterning, new horizons in (molecular) data storage are opened. We are given access to completely new avenues in view of alternative information processing technologies (e.g., cellular automata, quantum computing) [11]. If one considers each metal ion within the extended network as addressable (still) bistable data point with an averaged metal ion distance of ca. 2 nm, a functional MIN nanostructure would easily lead to data storage capacities in the several hundreds of Tb/in^2. This is clearly above the actual state-of-the-art of storage devices (below 1 Tb/in^2), but it is also more than what might be achievable by 2D monodomain cluster deposition (without organic molecules) on Au (788) surfaces (26 Tb/in^2) [40]. The additional use of the intrinsic multistability of metal ions through the ion dot concept would go beyond these numbers; this might be a strong motivation to implement molecular metal ion components into the nanoscale devices. However, the implementation and controlled exploitation of metal ion arrays (MIAs) and networks (MINs) within device architectures must find a way to bridge the gap between the molecular nano- and the environmental macrodimensions. Highly integrated carbon nanotube-electrode structures can act as the appropriate connector tool, linking the nanoworld of supramolecular metal ion assemblies with the macroscopic device environments. In sum, such molecule-based device geometries comprising (i) metal ion assemblies, (ii) carbon nanotubes, and (iii) nanostructured metallic electrodes would combine the advantages of both bottom-up self-assembly concepts and cutting-edge top-down fabrication techniques for the development of future information processing applications.

REFERENCES

1. N. C. Seemann. *Nature*, 421: pp 427–431, 2003.
2. R. F. Service. *Science*, 314: pp 1868–1870, 2006.
3. ENIAC-Strategic Research Agenda, European Technology Platform Nanoelectronics. Nov 2005. http://www.cordis.lu/ist/eniac.
4. J. M. Lehn. *Supramolecular Chemistry: Concepts and Perspectives*. Weinheim: VCH, 1995, Ch. 9; p 200.
5. J. Repp, G. Meyer, F. E. Olsson, and M. Person. *Science*, 305: pp 493–497, 2004.
6. C. S. Lent, B. Isaksen, and M. Lieberman. *Journal of American Chemistry Society*, 125: pp 1056–1063, 2003. M. Lieberman, S. Chellamma, B. Varughese, Y. Wang, C. Lent, G. H. Bernstein, G. Snider, and F. C. Peiris. *Annals of the New York Academy of Sciences*, 960: pp 225–239, 2002. A. O. Orlov, I. Amlani, G. H. Bernstein, C. S. Lent, and G. L. Snider*Science*, 277: pp 928–930,1997.
7. F. Meier, J. Levy, and D. Loss. *Physical Review Letters*, 90: p. 047901, 2003.
8. L. Kouwenhoven and C. Marcus. *Physics World*: pp 36–39, June 1998.
9. A. Landa and M. Ruben. In preparation.
10. M. Ruben, J. Rojo, F. J. Romero-Salguero, L. H. Uppadine, and J. M. Lehn. *Angewandte Chemie International Edition*. 43: pp 3644–3662, 2004.
11. S. Bertaina, S. Gambarelli, A. Tkashuk, I. N. Kurkin, B. Malkin, A. Stepanov, and B. Barbara. *Nature Nanotechnology*: 2: pp 39–42, 2007.
12. M. N. Leuenberger and D. Loss. *Nature*, 410: pp 789–794, 2001.
13. See some recent examples: (a) S. D. Feyter, and F. C. D. Schryver. *Chemical Society Reviews*, 32: pp 139–150, 2003; (b) P. Samorí. *Chemical Society Reviews*, 34: pp 551–561, 2005; (c) J. V. Barth, G. Costantini, and K. Kern. *Nature*, 437: pp 671–684, 2005.
14. (a) M. Ruben, E. Breuning, J. P. Gisselbrecht, and J. M. Lehn. *Angewandte Chemie International Edition*, 39: pp 4139–4142, 2000; (b) L. Zhao, C. J. Matthews, L. K. Thompson, and S. L. Heath. *Chemical Communications*: pp 265–266, 2000.
15. (a) M. Ruben, E. Breuning, M. Barboiu, J. P. Gisselbrecht, and J. M. Lehn. *Chemistry, A European Journal*, 9: pp 291–299, 2003; (b) D. M. Bassani, J. M. Lehn, S. Serroni, F. Puntoriero, and S. Campagna. *Chemistry, A European Journal*, 9: pp 5936–5946, 2003.
16. M. S. Alam, S. Strömsdorfer, V. Dremov, P. Müller, J. Kortus, M. Ruben, and J. M. Lehn. *Angewandte Chemie International Edition*, 117: pp 8109–8113, 2005.
17. L. H. Uppadine, J. P. Giesselbrecht, N. Kyritsakas, K. Nättinen, K. Rissanen, and J. M. Lehn. *Chemistry, A European Journal*, 11: pp 2549–2565, 2005.
18. O. Kahn and J. C. Martinez. *Science*, 279: pp 44–48, 1998.
19. P. Gütlich, A. Hauser, and H. Spiering. *Angewandte Chemie International Edition*, 33: pp 2024–2054, 1994.
20. (a) M. Ruben, U. Ziener, J. M. Lehn, V. Ksenofontov, P. Gütlich, and G. B. M. Vaughan. *Chemistry, A European Journal*, 11: pp 94–100, 2005; (b) M. Ruben,

E. Breuning, J. M. Lehn, V. Ksenofontov, F. Renz, P. Gütlich, and G. B. M. Vaughan. *Chemistry, A European Journal*, 9: pp 4422–4429, 2003; (c) E. Breuning, M. Ruben, J. M. Lehn, F. Renz, Y. Garcia, V. Ksenofontov, P. Gütlich, E. Wegelius, and K. Rissanen. *Angewandte Chemie International Edition*, 39: pp 2504–2507, 2000.

21. O. Waldmann, M. Ruben, U. Ziener, P. Müller, and J. M. Lehn. *Inorganic Chemistry*, 45: pp 6535–6540, 2006.
22. M. Ruben. *Angewandte Chemie International Edition*, 44: pp 1594–1596, 2005.
23. (a) A. Semenov, J. P. Spatz, M. Möller, J. M. Lehn, B. Sell, D. Schubert, C. H. Weidl, and U. S. Schubert. *Angewandte Chemie International Edition*, 38: pp 2547–2550, 1999; (b) U. Ziener, J. M. Lehn, A. Mourran, and M. Möller. *Chemistry, A European Journal*, 8: pp 951–957, 2002.
24. J. Hassmann, C. Y. Hahn, O. Waldmann, E. Volz, H. J. Schleemilch, N. Hallschmid, P. Müller, G. S. Hanan, D. Volkmer, U. S. Schubert, J. M. Lehn, H. Mauser, A. Hirsch, and T. Clark. *Materials Research Society Symposium Proceedings*, 488: pp 447–452, 1988.
25. (a) L. Weeks, L. K. Thompson, J. G. Shapter, K. J. Pope, and Z. Xu. *Journal of Microscopy*, 212: pp 102–106, 2003; (b) V. A. Milway, S. M. Tareque Abedin, V. Niel, T. L. Kelly, L. N. Dawe, S. K. Dey, D. W. Thompson, D. O. Miller, M. S. Alam, P. Müller, and L. K. Thompson. *Dalton Transactions:* pp 2835–2851, 2006.
26. M. Ruben, J. M. Lehn, and P. Müller. *Chemical Society Reviews*, 35: pp 1056–1067, 2006.
27. N. Lin, S. Stepanow, F. Vidal, K. Kern, M. S. Alam, S. Stromsdörfer, V. Dremov, P. Müller, A. Landa, and M. Ruben. *Dalton Transactions*: pp 2794–2800, 2006.
28. N. Lin, S. Stepanow, F. Vidal, K. Kern, M. S. Alam, S. Stromsdörfer, V. Dremov, P. Müller, A. Landa, and M. Ruben. *Dalton Transactions*: pp 2794–2800, 2006.
29. A. P. Seitsonen, M. A. Lingenfelder, H. Spillmann, A. Dmitriev, S. Stepanow, N. Lin, K. Kern, and J. V. Barth. *Journal of American Chemistry Society*, 128: pp 5634–5635, 2006.
30. L. Lin, S. Stepanow, F. Vidal, J. V. Barth, and K. Kern. *Chemical Communications*, 13: pp 1681–1683, 2005.
31. S. Stepanow, N. Lin, D. Payer, U. Schlickum, F. Klappenberger, G. Zappellaro, M. Ruben, H. Brune, J. V. Barth, and K. Kern. *Angewandte Chemie International Edition*, 46: pp 710–713, 2007.
32. W. Auwärter, A. Weber-Bargioni, S. Brink, A. Riemann, A. Schiffrin, M. Ruben, and J. V. Barth. *ChemPhysChem*, 8: pp 250–254, 2007.
33. Y. Yan, M. B. Chan-Park, and Q. Zhang. *Small*, 3: pp 24–42, 2007.
34. (a) S. Sun, C. B. Murray, D. Weller, L. Folks, and A. Moser. *Science*, 287: pp 1989–1992, 2000; (b) Y. Yang, S. Huang, H. He, A. W. H. Mau, and L. Dai. *Journal of American Chemistry Society*, 121: pp 10832–10833, 1999.
35. H. Lui, S. Li, J. Zhai, H. Li, Q. Zheng, L. Jiang, and D. Zhu. *Angewandte Chemie International Edition*, 43: pp 1146–1149, 2004.
36. S. J. Tans, M. H. Devoret, H. J. Dai, A. Thess, R. E. Smalley, L. J. Geerlings, and C. Dekker. *Nature*, 386: pp 474–477, 1997.
37. R. Krupke, F. Hennrich, H. B. Weber, M. M. Kappes, and H. von Loehneysen. *Nano Letters*, 3: pp 1019–1022, 2003.

38. P. Jarillo-Herrero, J. A. van Dam, and L. P. Kouwenhouven. *Nature*, 439: pp 953–956, 2006.
39. J. P. Cleuziou, W. Wernsdorfer, V. Bouchiat, T. Ondarcuhu, and M. Monthiuox. *Nature Nanotechnology*, 1: pp 53–59, 2006.
40. N. Weiss, T. Cren, M. Epple, S. Rusponi, G. Baudot, S. Rohart, A. Tejeda, V. Repain, S. Rousset, P. Ohresser, F. Scheurer, P. Bencok, and H. Brune. *Physical Review Letters*, 95: pp 157–204, 2005.